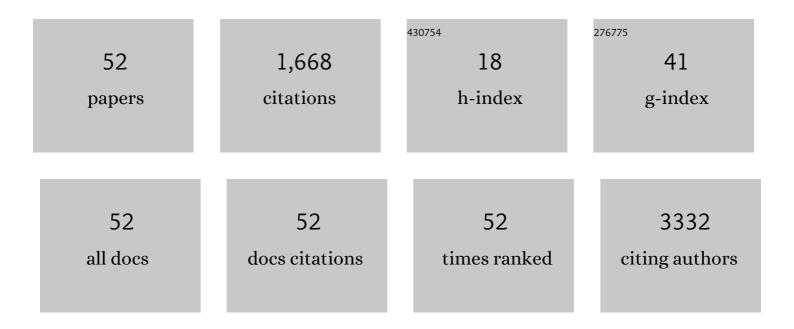
Li Wang

List of Publications by Year in descending order

Source: https://exaly.com/author-pdf/918437/publications.pdf Version: 2024-02-01



#	Article	IF	CITATIONS
1	Recent advances in understanding of the mechanism and control of Li ₂ O ₂ formation in aprotic Li–O ₂ batteries. Chemical Society Reviews, 2017, 46, 6046-6072.	18.7	314
2	Electron-Doping-Enhanced Trion Formation in Monolayer Molybdenum Disulfide Functionalized with Cesium Carbonate. ACS Nano, 2014, 8, 5323-5329.	7.3	211
3	Waterâ€Catalyzed Oxidation of Few‣ayer Black Phosphorous in a Dark Environment. Angewandte Chemie - International Edition, 2017, 56, 9131-9135.	7.2	141
4	Surface Functionalization of Black Phosphorus via Potassium toward High-Performance Complementary Devices. Nano Letters, 2017, 17, 4122-4129.	4.5	117
5	Growth of Quasi-Free-Standing Single-Layer Blue Phosphorus on Tellurium Monolayer Functionalized Au(111). ACS Nano, 2017, 11, 4943-4949.	7.3	109
6	Growth of Millimeter-Size Single Crystal Graphene on Cu Foils by Circumfluence Chemical Vapor Deposition. Scientific Reports, 2014, 4, 4537.	1.6	98
7	Artificial Multiferroics and Enhanced Magnetoelectric Effect in van der Waals Heterostructures. ACS Applied Materials & Interfaces, 2020, 12, 6243-6249.	4.0	81
8	Two-dimensional black phosphorus: its fabrication, functionalization and applications. Nanoscale, 2018, 10, 21575-21603.	2.8	73
9	Implanting cation vacancies in Ni-Fe LDHs for efficient oxygen evolution reactions of lithium-oxygen batteries. Applied Catalysis B: Environmental, 2021, 285, 119792.	10.8	56
10	Oxygen induced strong mobility modulation in few-layer black phosphorus. 2D Materials, 2017, 4, 021007.	2.0	45
11	Abnormal Nearâ€Infrared Absorption in 2D Black Phosphorus Induced by Ag Nanoclusters Surface Functionalization. Advanced Materials, 2018, 30, e1801931.	11.1	43
12	Defect Chemistry in Discharge Products of Li–O ₂ Batteries. Small Methods, 2019, 3, 1800358.	4.6	34
13	Improvement of the electrochemical performance of Li1.2Ni0.13Co0.13Mn0.54O2 cathode material by Al2O3 surface coating. Journal of Electroanalytical Chemistry, 2020, 859, 113845.	1.9	30
14	Chiral recognition of zinc phthalocyanine on Cu(100) surface. Applied Physics Letters, 2012, 100, 081602.	1.5	28
15	Metal Induced Growth of Transition Metal Dichalcogenides at Controlled Locations. Scientific Reports, 2016, 6, 38394.	1.6	28
16	Switching Molecular Orientation of Individual Fullerene at Room Temperature. Scientific Reports, 2013, 3, 3062.	1.6	27
17	Modulation of Coordinate Bonds in Hydrogen-Bonded Trimesic Acid Molecular Networks on Highly Ordered Pyrolytic Graphite Surface. Journal of Physical Chemistry C, 2016, 120, 12605-12610.	1.5	23
18	Direct observation of copper-induced metalation of 5,15-diphenylporphyrin on Au(111) by scanning tunneling microscopy. Surface Science, 2015, 633, 46-52.	0.8	18

LI WANG

#	Article	IF	CITATIONS
19	Self-assembly of hydrogen-bonded supramolecular complexes of nucleic-acid-base and fatty-acid at the liquid–solid interface. Physical Chemistry Chemical Physics, 2016, 18, 14168-14171.	1.3	18
20	Cyclotrimerizationâ€Induced Chiral Supramolecular Structures of 4â€Ethynyltriphenylamine on Au(111) Surface. Chemistry - A European Journal, 2015, 21, 12978-12983.	1.7	17
21	Promoting defective-Li ₂ O ₂ formation <i>via</i> Na doping for Li–O ₂ batteries with low charge overpotentials. Journal of Materials Chemistry A, 2019, 7, 10389-10396.	5.2	17
22	Structural Transformation of Guanine Coordination Motifs in Water Induced by Metal lons and Temperature. Langmuir, 2018, 34, 8092-8098.	1.6	16
23	Confining Li2O2 in tortuous pores of mesoporous cathodes to facilitate low charge overpotentials for Li-O2 batteries. Journal of Energy Chemistry, 2021, 55, 55-61.	7.1	16
24	Chiral supramolecular self-assembly of rubrene. Physical Chemistry Chemical Physics, 2010, 12, 14682.	1.3	14
25	On-Surface Synthesis of Chiral π-Conjugate Porphyrin Tapes by Substrate-Regulated Dehydrogenative Coupling. Journal of Physical Chemistry C, 2019, 123, 23007-23013.	1.5	14
26	Highly ordered arrays and characterization of WS2 flakes grown by low pressure chemical vapour deposition. Chemical Physics, 2019, 523, 106-109.	0.9	9
27	Recent advances in charge mechanism of noble metal-based cathodes for Li-O2 batteries. Chinese Chemical Letters, 2023, 34, 107413.	4.8	9
28	Construction of a Molecular Switch Based on Two Metastable States of Fullerene on Cu(111). Journal of Physical Chemistry C, 2020, 124, 11158-11164.	1.5	6
29	Surface-assisted dehydrogenative homocoupling and cyclodehydrogenation of mesityl groups on a copper surface. Chemical Communications, 2017, 53, 9151-9154.	2.2	5
30	Observations of carbon–carbon coupling of 4,4ʺ-dibromo- p -terphenyl on Cu(110) surface at molecular level. Chinese Chemical Letters, 2017, 28, 24-28.	4.8	5
31	Surface-mediated construction of diverse coordination-dominated nanostructures with 4-azidobenzoic acid molecule. Journal of Chemical Physics, 2020, 152, 044704.	1.2	5
32	Growth of few-layer graphene on Cu foil by regulating the pressure of reaction gases. CrystEngComm, 2020, 22, 1018-1023.	1.3	5
33	Hot-carrier infrared detection in PbS with ultrafast and highly sensitive responses. Applied Physics Letters, 2022, 120, .	1.5	5
34	Patterned growth of tungsten diselenide flakes by chemical vapor deposition. Japanese Journal of Applied Physics, 2017, 56, 080303.	0.8	4
35	Flexible current collector–free LiFePO4/carbon composite film for high-performance lithium-ion batteries. Ionics, 2019, 25, 939-947.	1.2	4
36	An approach to high-throughput growth of submillimeter transition metal dichalcogenide single crystals. Nanoscale, 2019, 11, 22440-22445.	2.8	4

LI WANG

#	Article	IF	CITATIONS
37	Synthesis of ordered conjugated polycyclic aromatic hydrocarbon polymers through polymerization reaction on Au(111). Chemical Communications, 2016, 52, 8420-8423.	2.2	3
38	Direct on-surface synthesis of gold–phthalocyanine <i>via</i> cyclization of cyano-groups with gold adatoms. Materials Chemistry Frontiers, 2019, 3, 1406-1410.	3.2	3
39	Direct observation of copper-induced role on Ullmann reaction by scanning tunneling microscopy. Chemical Physics, 2019, 522, 65-68.	0.9	3
40	Transformation of the coordination nanostructures of 4,4′,4′′-(1,3,5-triazine-2,4,6-triyl) tribenzoic acid molecules on HOPG triggered by the change in the concentration of metal ions. RSC Advances, 2022, 12, 3892-3896.	1.7	3
41	Assembling fullerene into nanostructures over micrometer scale with atomic precision. Nanotechnology, 2018, 29, 395301.	1.3	2
42	CVD growth of rhenium sulfide on carbon nanotubes as an anode for improving the performance of lithium ion batteries. Nanotechnology, 2021, 32, 155703.	1.3	1
43	Enhanced luminescence of Si(111) surface by localized surface plasmons of silver islands. Nanotechnology, 2021, 32, 295204.	1.3	1
44	General synthesis of mixed-dimensional van der Waals heterostructures with hexagonal symmetry. Nanotechnology, 2021, 32, 505610.	1.3	1
45	Directing on-surface polymerization via substrate-directed molecular template. Physical Chemistry Chemical Physics, 2022, , .	1.3	1
46	All-Optical Reconfigurable Electronic Memory in a Graphene/SrTiO ₃ Heterostructure. ACS Omega, 2022, 7, 15841-15845.	1.6	1
47	Observations of Gradual Chiral Self-Recognition of Adsorbed Aromatic Compound. Langmuir, 2019, 35, 870-874.	1.6	0
48	Direct observation of meta-selective C-H activation on Pd(1 1 1) by scanning tunneling microscopy. Chemical Physics, 2020, 539, 110981.	0.9	0
49	Polymorphic Pairing Configurations of Guanine and Cytosine at the Water–HOPG Interface. Langmuir, 2021, 37, 3761-3765.	1.6	0
50	Passive Electronic Skin with Highly Sensitive Tactile Sensory Capabilities. ACS Applied Electronic Materials, 0, , .	2.0	0
51	A current collect-free Li _{1.2} Ni _{0.13} Co _{0.13} Mn _{0.54} O ₂ flexible film for high-performance lithium-ion batteries. Nanotechnology, 2022, 33, 045703.	1.3	0
52	Three-Bit Digital Comparator Based on Intracell Diffusion of Silver Single Atom. Nano Letters, 2022, 22, 5909-5915.	4.5	0